Utilizing potential field data to support delineation of groundwater aquifers in the southern Red Sea coast, Saudi Arabia

Article *in* Journal of Geophysics and Engineering · June 2012

DOI: 10.1088/1742-2132/9/3/327

CITATIONS
2

READS
303

5 authors, including:

Eslam Ahmed Elawadi
King Saud University
55 PUBLICATIONS **316** CITATIONS
SEE PROFILE

Saad Mogren
King Saud University
40 PUBLICATIONS **411** CITATIONS
SEE PROFILE

Awni T Batayneh
King Saud University
70 PUBLICATIONS **716** CITATIONS
SEE PROFILE

Abdulaziz Al Bassam
King Saud University
42 PUBLICATIONS **228** CITATIONS
SEE PROFILE

Some of the authors of this publication are also working on these related projects:

Geothermal View project

geography View project

Utilizing potential field data to support delineation of groundwater aquifers in the southern Red Sea coast, Saudi Arabia

2012 J. Geophys. Eng. 9 327

(http://iopscience.iop.org/1742-2140/9/3/327)

IOP Publishing Journal of Geophysics and Engineering
J. Geophys. Eng. **9** (2012) 327–335 doi:10.1088/1742-2132/9/3/327

Utilizing potential field data to support delineation of groundwater aquifers in the southern Red Sea coast, Saudi Arabia

Eslam Elawadi[1,2], Saad Mogren[1], Elkhedr Ibrahim[1,3], Awni Batayneh[1] and Abdulaziz Al-Bassam[1]

[1] Department of Geology and Geophysics, King Saud University, Riyadh, Kingdom of Saudi Arabia
[2] Nuclear Materials Authority, Cairo, Egypt
[3] Earth Sciences Department, Faculty of Science, Mansoura University, Egypt

E-mail: eelawadi@ksu.edu.sa and eibrahim@ksu.edu.sa

Received 15 October 2011
Accepted for publication 24 April 2012
Published 24 May 2012
Online at stacks.iop.org/JGE/9/327

Abstract
In this paper potential field data are interpreted to map the undulation of the basement surface, which represents the bottom of the water bearing zones, and to delineate the tectonic framework that controls the groundwater flow and accumulation in the southern Red Sea coastal area of Saudi Arabia. The interpretation reveals that the dominant structural trend is a NW (Red Sea) trend that resulted in a series of faulted tilted blocks. These tilted blocks are dissected by another cross-cut NE trend which shapes and forms a series of fault-bounded small basins. These basins and the bounded structural trends control and shape the flow direction of the groundwater in the study area, i.e. they act as groundwater conduits. Furthermore, the present results indicate that volcanic intrusions are present as subsurface flows, which hinder the groundwater exploration and drilling activities in most of the area; in some localities these volcanic flows crop out at the surface and cover the groundwater bearing formations. Furthermore, the gravity and magnetic data interpretation indicates the possible existence of a large structural basin occupying the southeastern side of the study area. This basin is bounded with NW and NE trending faults and is expected to be a good host for groundwater aquifers; thus it is a promising site for hydrogeological investigation.

Keywords: magnetic, gravity, groundwater, Saudi Arabia

(Some figures may appear in colour only in the online journal)

1. Introduction

The study area is a coastal zone in the southwestern corner of Saudi Arabia, which is located between latitudes 17° and 19° N and longitudes 40° to 43° E (figure 1). This zone comprises many highly populated urban areas. Although the relatively high precipitation rate (200–600 mm year^{-1}) at the Assir Mountains, which includes the study area, the region is considered to be water scarce. Groundwater exploration and management in such arid areas causes a great deal of concern because of the increasing demand for additional sustainable water resources to satisfy demographic growth and economic development. However, the required subsurface information for groundwater assessment and management are not available due to limited geophysical/hydrological studies of the area.

The area has been covered by airborne magnetic surveys in different phases (1962–1983) using different survey specifications. Hunting Geology and Geophysics Ltd supervised by USGS flew over the southern part of the study area in 1962 using the Fluxgate Gulf Mark III magnetometer with analogue recording. Terrain clearance was 300 m, traverse direction was N55E and the traverse spacing was 1250 m. The northern part of the study area was flown over in 1966–1967 by a consortium of four corporations (Aero Service Corp.,

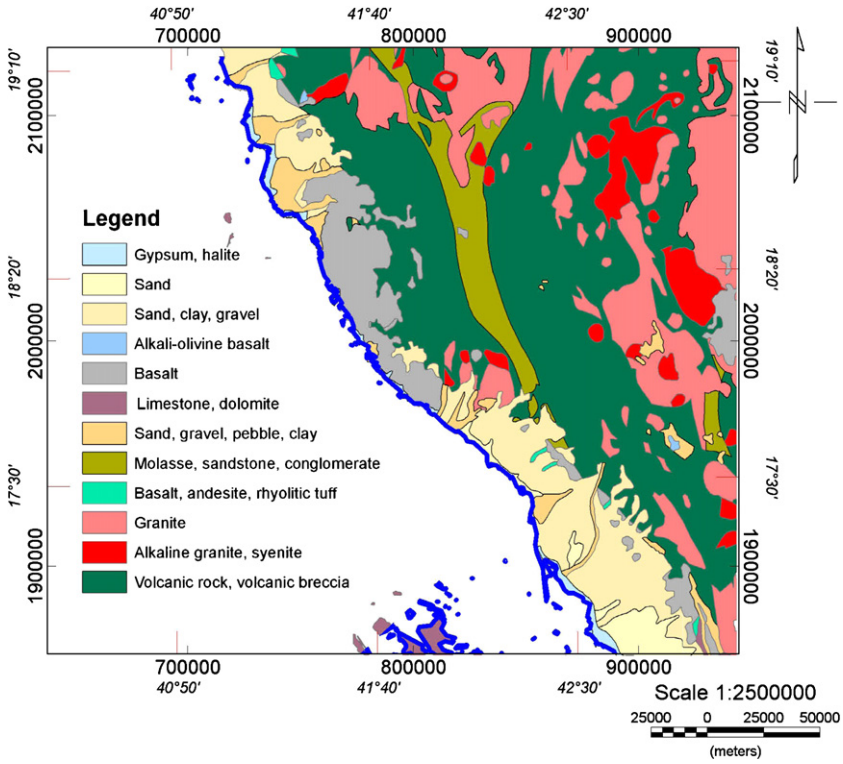

Figure 1. Geologic map of the study area (reproduced from Blank *et al* 1985, Greenwood 1985, Prinz 1984 and Fairer 1985).

Hunting Geology and Geophysics Ltd, Lockwood Survey Corporation Ltd and ARGAS) using the Fluxgate Gulf Mark III magnetometer with analogue recording. Terrain clearance was 300 m, traverse direction was N30E and the traverse spacing was 800 m. The coastal plain of the study area was flown over in 1983 by Geo-Survey International Ltd under the supervision of USGS with a terrain clearance of 300 m, a traverse direction of N30E, and a traverse spacing of 2000 m using the Geometrics G813 Proton precession magnetometer with digital recording. For the southern part of the study area, the Saudi Geological Survey (SGS) collected the data in 1985 in one grid after applying data levelling and grid knitting.

Moreover, a ground gravity survey was conducted for the study area by the US Geological Survey (USGS), a Saudi Arabian mission in Jeddah, during the period from October 1974 to December 1977. The LaCoste-Romberg geodetic gravimeter was used and the survey was tied to a gravity base station, normally within three hours. The survey was done at a nominal spacing of one station per 10 km^2. The overall estimated errors were ± 50 m for position and ± 0.7 mGal for the gravity values.

2. General geology

The study area is covered with rock units ranging in age from Proterozoic to Cenozoic (figure 1). The Proterozoic rocks cover the eastern part of the study area and are present in the form of meta-sediments and meta-volcanics which are represented mainly by the Sabya Formation, Baish and the Abha groups (Blank *et al* 1985). The Palaeozoic and Mesozoic rocks are mainly sandstone and are represented mainly by the Wajid Formation in the study area. The Cenozoic era is represented by Tertiary and Quaternary basalts and alluvial Quaternary deposits. The study area is intruded in different places by different intrusions, ranging in age from Proterozoic to Cenozoic and in lithology from grandoirite to diorite, gabbro and basalt. Pleistocene to Holocene deposits are widely spread especially along the coastal plain, including raised terraces, reef limestone, Quaternary sand, alluvial deposits, gravel and some recent evaporates.

From the Cambrian through to the Quaternary period, the area has been subjected to different tectonic activities which were accentuated with the opening of the Red Sea (Oligo–Miocene). The prominent structural features in the area fault trend in the NW–SE and NW–SE directions forming elongated grabens and horsts (Mogren *et al* 2011 and Basahel *et al* 1983). The main wadies in the study area trend from west to east, generally following the main fracture system (Hussain and Ibrahim 1997).

3. Data analysis

High-resolution aeromagnetic data is used here as a basis for mapping and delineating the structural architecture that effects and controls the groundwater aquifers in the study area. The total magnetic intensity (figure 2) was reduced to the pole (RTP) to overcome the bipolarity phenomena of the magnetic data (figure 3). However, reduction to the pole of such a low latitude area requires special care to reduce the blow-up of the north–south features. Known as amplitude correction, this inconvenience can be eliminated by specifying a higher latitude for the amplitude correction alone, at the expense of under-correcting the amplitudes of the north–south features.

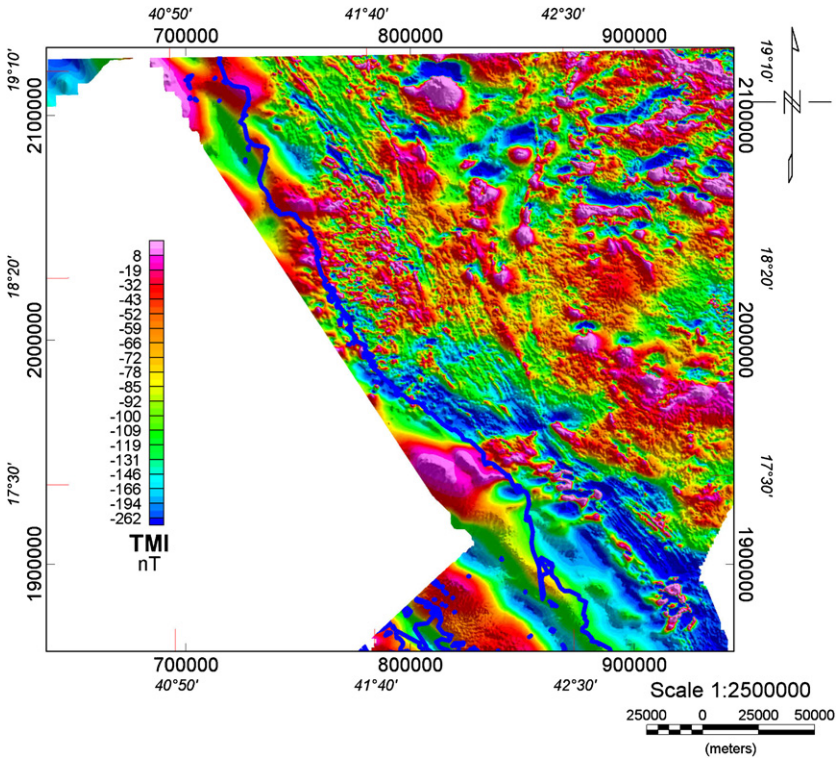

Figure 2. Total intensity magnetic map (TMI).

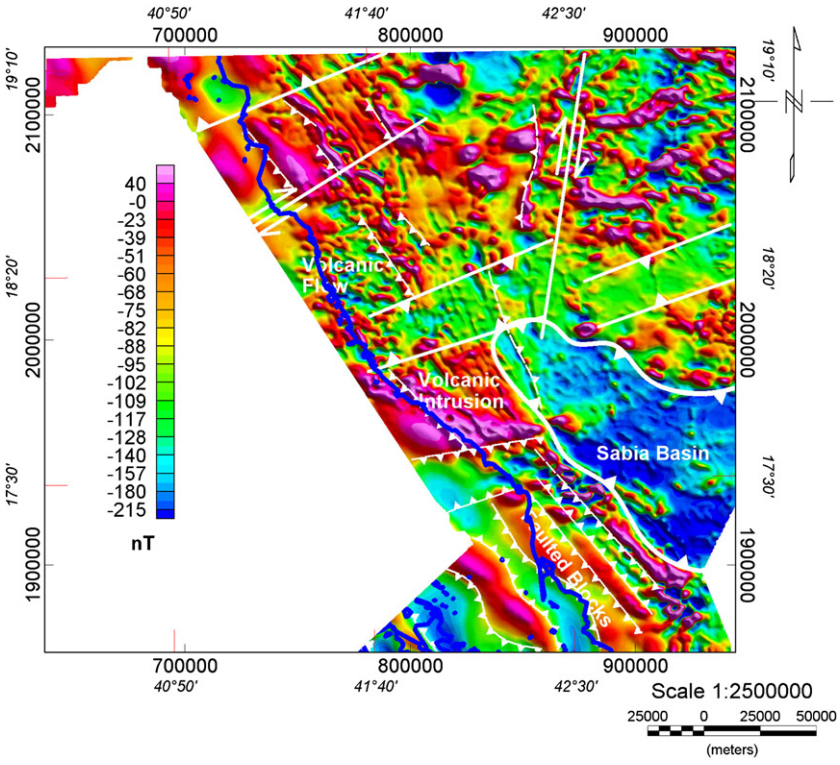

Figure 3. RTP total magnetic intensity map of the area.

In order to achieve the main objective of the study, several filters are used. The objective of these filters is to condition the data set and to render the resulting presentation in such a way as to make it is easier to interpret the significance of anomalies in terms of their geological sources (Bird 1997). Therefore, the most effective way to filter the data is with an understanding of the geological control and the desired filtered results. Several filtering techniques can be performed in the frequency domain. However, one of the most traditional filters, used in the potential field, is the separation of long (deep) and short (shallow) wavelength anomalies. The cut-off wavelengths and information about the contribution of the

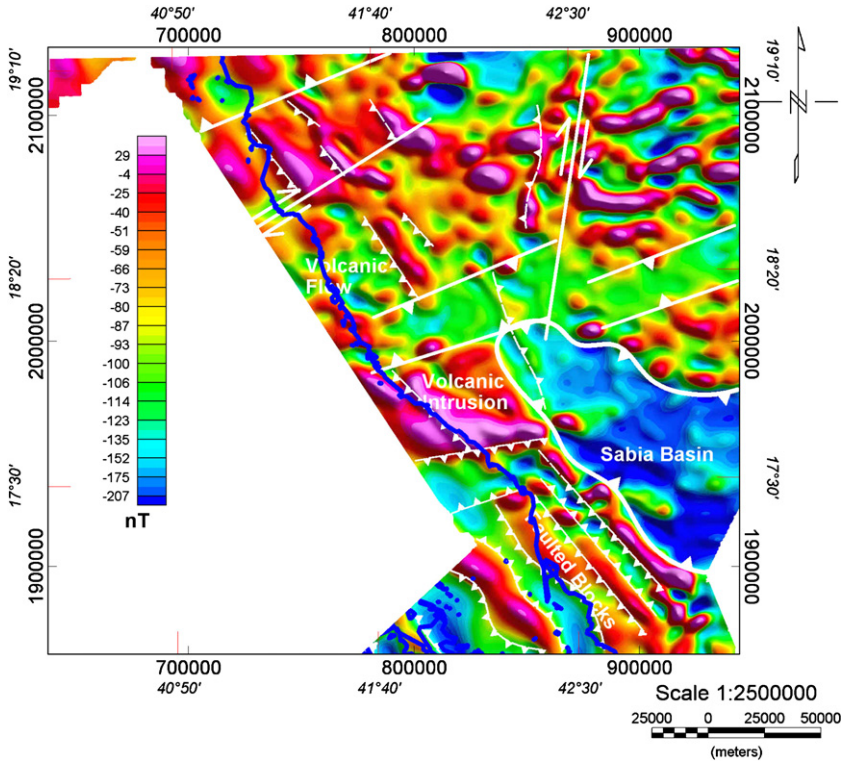

Figure 4. The regional magnetic anomaly map.

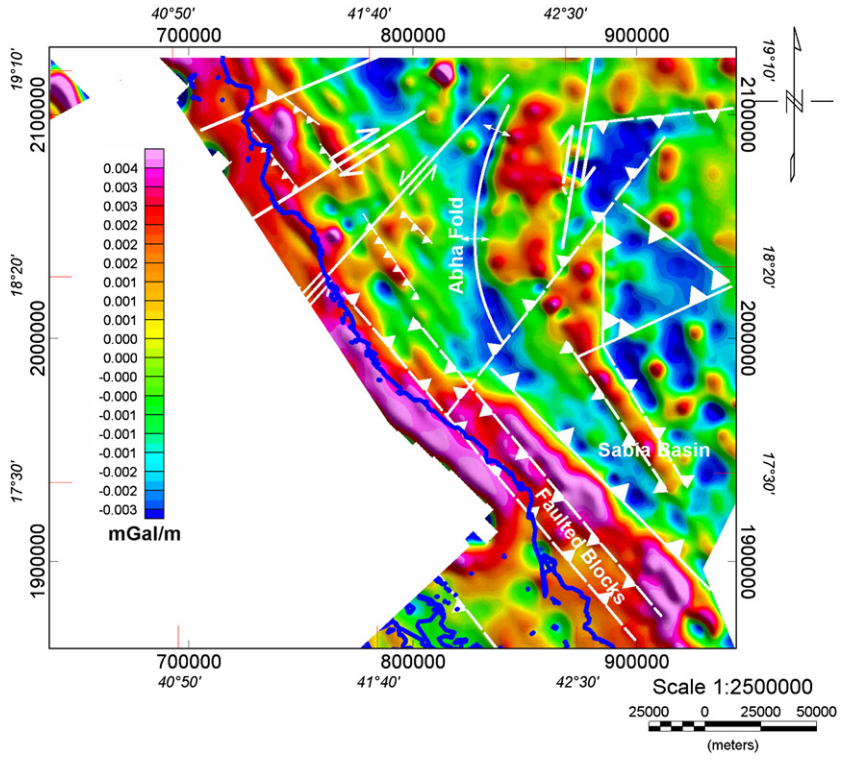

Figure 5. First vertical derivative of the Bouguer gravity anomaly map.

short and long wavelengths in the spectrum can be obtained from the calculated radially-averaged power spectrum of the data. The RTP data were separated into regional (figure 4) and residual components through an application of the Butterworth filter technique, using a central wave number of 0.09 and degree 8.

To enhance the mapping of the basaltic flow and near-surface intrusions, a further first horizontal derivative, a second vertical derivative and an analytic signal were applied to the RTP residual map to produce the enhanced residual map (figure 6). The map is self-explanatory and clearly shows the spatial distribution of the surface and near-surface volcanic

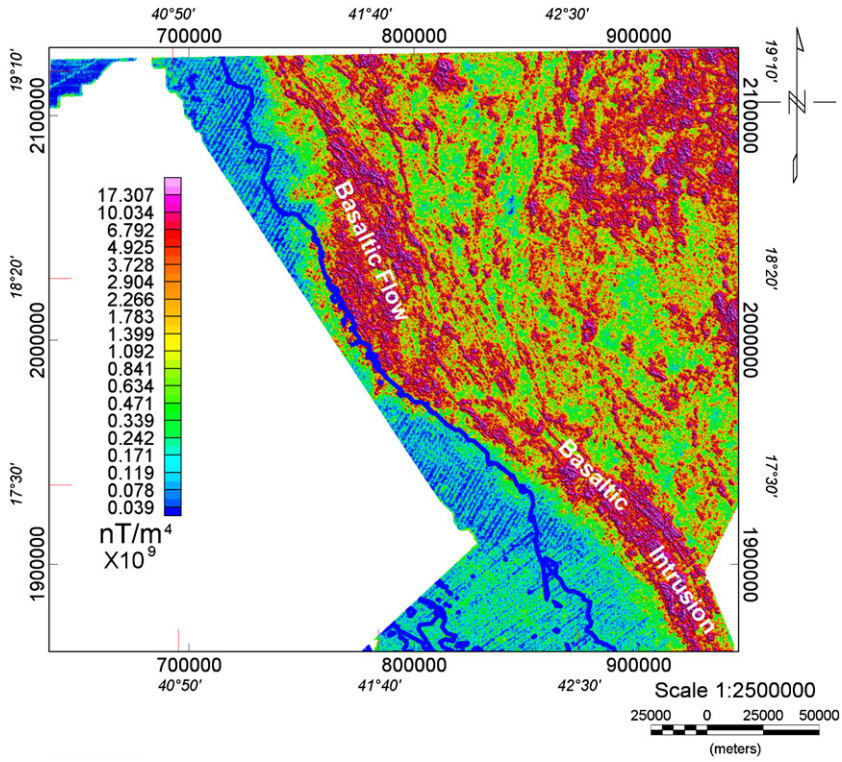

Figure 6. Enhanced residual magnetic anomaly map.

intrusions. The regional magnetic map reveals the deeper compositions and structures of the study area and can be used for further depth estimations and source mapping techniques. On the other hand, the gravity data were filtered, using both a low-pass filter and the first vertical derivative, to enhance the signal related to the near-surface geological structures. Both maps show comparable features and map the faulted blocks (grabens and horsts) elongated parallel to the Red Sea trend.

4. Interpretation techniques

Three automatic interpretation techniques were applied to delineate the structures from the RTP magnetic and Bouguer gravity anomaly data. The general requirement for an automatic lineament detection algorithm is the transformation of the data such that the edge of a causative body is located beneath a maximum in the grid. Several automatic interpretation techniques satisfy this requirement, e.g. horizontal derivative (HD), source edge detection (SED) and Euler deconvolution (ED). The horizontal gradient method has been used intensively to locate contacts of density contrast from the gravity data (Cordell 1979). The advantages of the horizontal gradient method are the low susceptibility to the noise and robustness to delineate either shallow or deep structures (Phillips (1998)). For the gravity field $G(x, y)$, the horizontal gradient magnitude $HG(x, y)$ is given by

$$HG(x, y) = \sqrt{\left(\frac{\partial G}{\partial x}\right)^2 + \left(\frac{\partial G}{\partial y}\right)^2}. \quad (1)$$

A grid of the total horizontal gradient computed from the Bouguer gravity display peaks over the edges of source bodies. These peaks can be picked up using the Blakely and Simpson (1986) method.

The SED method calculates the TDX (arctan(total_horizontal_gradient/first_vertical_derivative) grid from the input RTP or gravity data. The positive peak values in the TDX grid are then extracted to locate the source's edges, using the Blakely and Simpson method, to define the source boundaries in vector format (i.e. to define its strike and dip, (see figures 7 and 8)).

Euler deconvolution (Reid *et al* (1990) and Thompson 1982) is an automatic technique used for locating the source of potential fields based on both their amplitudes and gradients. A 3D form of Euler's equation can be defined as

$$x_0\frac{\partial g}{\partial x} + y_0\frac{\partial g}{\partial y} + z_0\frac{\partial g}{\partial z} + NB = x\frac{\partial g}{\partial x} + y\frac{\partial g}{\partial y} + z\frac{\partial g}{\partial z} + Ng, \quad (2)$$

where $\partial g/\partial x$, $\partial g/\partial y$ and $\partial g/\partial z$ are the derivatives of the field in the x, y and z directions, B is a constant term describing the background field and N is the structural index value that needs to be chosen according to a prior knowledge of the source geometry. By considering four or more neighbouring observations at a time (an operated window), the source location (x_0, y_0, z_0) and B can be computed by solving a linear system of equations generated from equation (2). Then, by moving the operating window from one location to the next over the whole anomaly, multiple solutions for the same source are obtained. This method was applied to the magnetic and the first derivative of gravity data (figure 9) to locate the source's edges in a 3D space using the step model (SI = 0.0). Appropriate windowing techniques are applied to retain the most sensible solutions. The method was applied to the regional magnetic and the first vertical derivative of the gravity data.

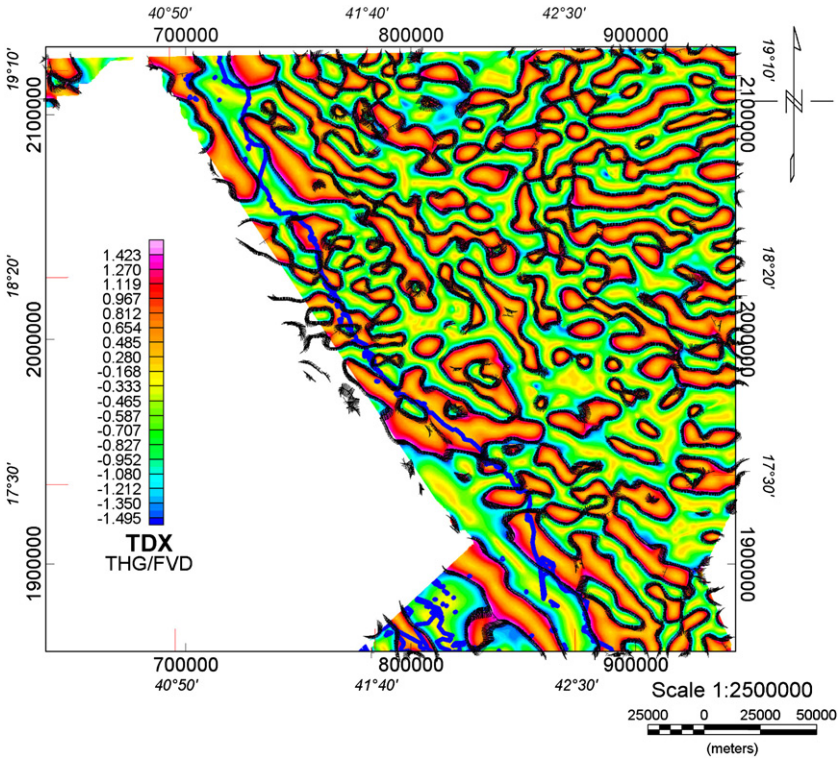

Figure 7. Source edge detection (SED) for the regional magnetic map (indicated as black boundaries of TDX maxima) overlies the TDX map (the background grid).

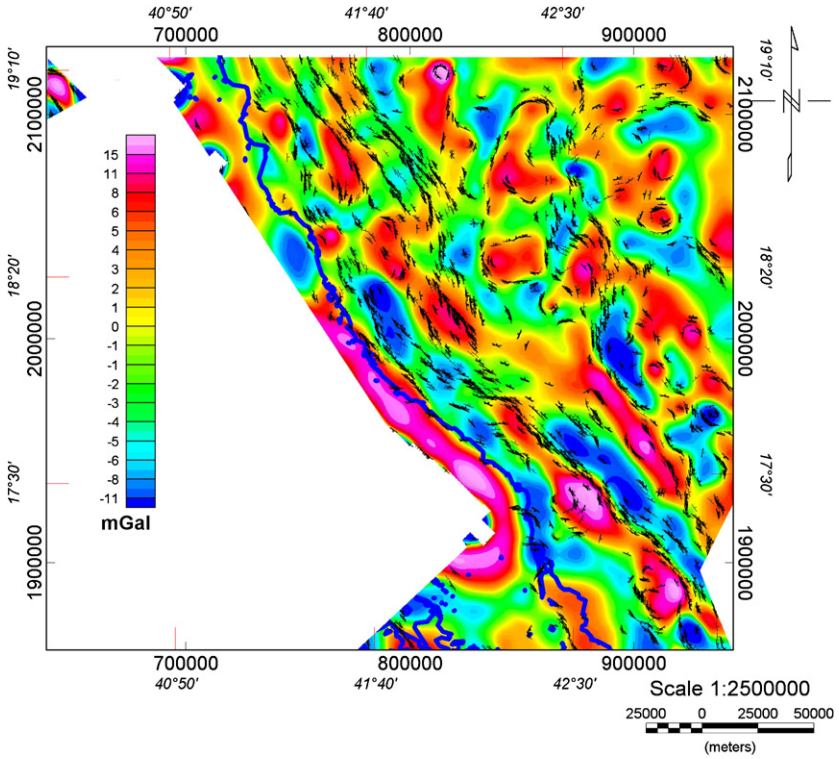

Figure 8. Source edge detection (SED) solutions (indicated as black dashes) overly the high-pass filtered gravity map (the background grid).

The local wave number (SPI) method is a technique based on the extension of complex analytical signals to estimate magnetic depths. The original SPI method (Smith *et al* (1998)) works for two models: a 2D sloping contact or a 2D dipping thin-sheet. For the magnetic field M, the local wave number (Smith *et al* 1998) is given by

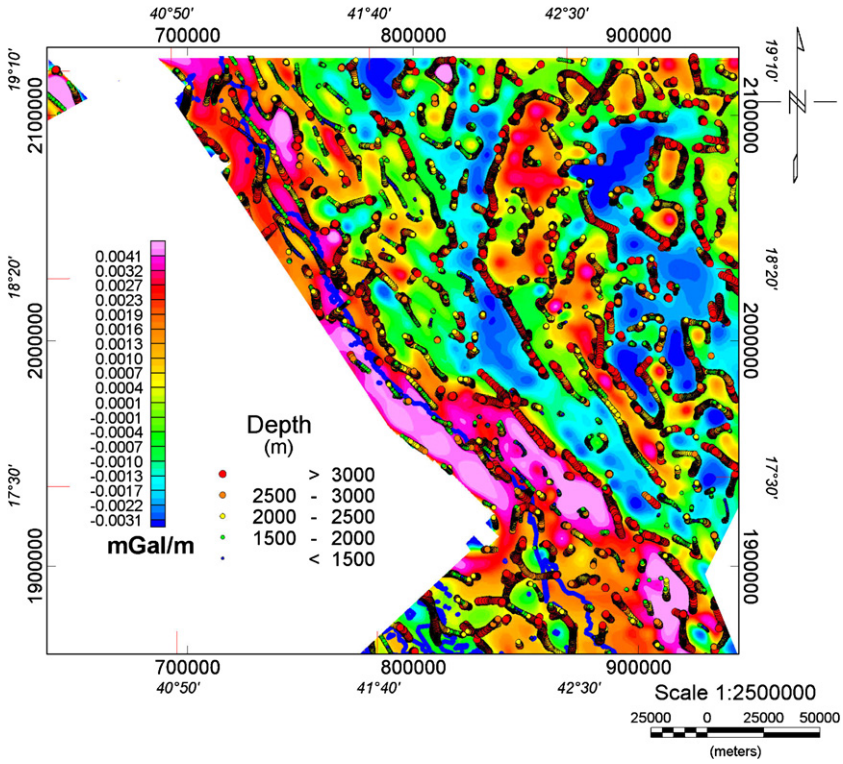

Figure 9. Euler solutions (SI = 0.0) for the first vertical derivative gravity map (the background grid).

$$k = \frac{\frac{\partial^2 M}{\partial x \partial z}\frac{\partial M}{\partial x} - \frac{\partial^2 M}{\partial x^2}\frac{\partial M}{\partial z}}{\left(\frac{\partial M}{\partial x}\right)^2 + \left(\frac{\partial M}{\partial z}\right)^2}. \quad (3)$$

For the dipping contact, the maxima of k are located directly over the isolated contact edges and are independent of the magnetic inclination, declination, dip, strike and any remnant of magnetization. The depth is estimated at the source's edge from the reciprocal of the local wave number:

$$\text{Depth}_{(x=0)} = \frac{1}{k_{\max}}. \quad (4)$$

One more advantage of this method is that the interference of anomaly features is reducible, since the method uses second-order derivatives. The peaks of SPI functions were traced by passing a small 3 × 3 window over the grid data and searching for maxima (Blakely and Simpson 1986). These maximum values are then put into a grid and displayed as a coloured depth map, as shown in figure 10.

5. Discussion and interpretation

Special attention is given here to a joint interpretation of the gravitational and magnetic data in the study area which were intruded by the different forms of basaltic flow, ranging from intra-basement, near-basement, surface flow or near-surface localized intrusions.

As a part of the Red Sea rift, the outcropping of basement rocks in the eastern part generally dip to the west through a set of faulted tilted blocks, which form a sequence of elongated grabens and horsts parallel to the Red Sea (Mogren *et al* 2011). This phenomenon is clearly revealed as a dominant NW trending anomaly in the regional magnetic map (figure 4) and in the first vertical derivative gravity maps (figure 5). This NW structure is dissected by cross-cut NNE–SSW and NE–SW trending faults that disfigure and truncate the NW structures. The alignment of the interpreted source edges (figures 7 and 8) confirms this conclusion and reveals that the two major trends affecting the study area are NW–SE and NE–SW. It is important to mention that the NE trend controls most of the surface drainage in the western side of the study area (e.g. Wadi Assir).

To the north of the study area there is an indication of a NNW fault that brings the folded Abha group to the surface. The signature of this fault is obvious in the magnetic maps (e.g. figures 3 and 4). However, in the magnetic maps there is no indication of folding in spite of the good representation of this fold in the filtered high-pass and the first vertical derivative Bouguer gravity maps (figure 5), as an elongated negative gravity anomaly extends about 100 km in the NNW direction with an average width of 12 km. This information indicates that the fold could affect the sedimentary cover and intact the basement rocks. This group is interrupted and cut in its southern side by an EW volcanic intrusion, most probably of Tertiary basalt, as indicated in the RTP map by a relatively extended EW high amplitude and low frequency magnetic anomaly (figure 3). This volcanic intrusion crops out at the surface in localities near to Wadi Ramlan, as confirmed by the field visits where it is extended to a great depth, as indicated by a clear high anomaly in the regional magnetic map (figure 4). The enhanced residual magnetic map (figure 8) clearly reveals how the spatial distribution of the volcanic flow affects the western side of the study area. These

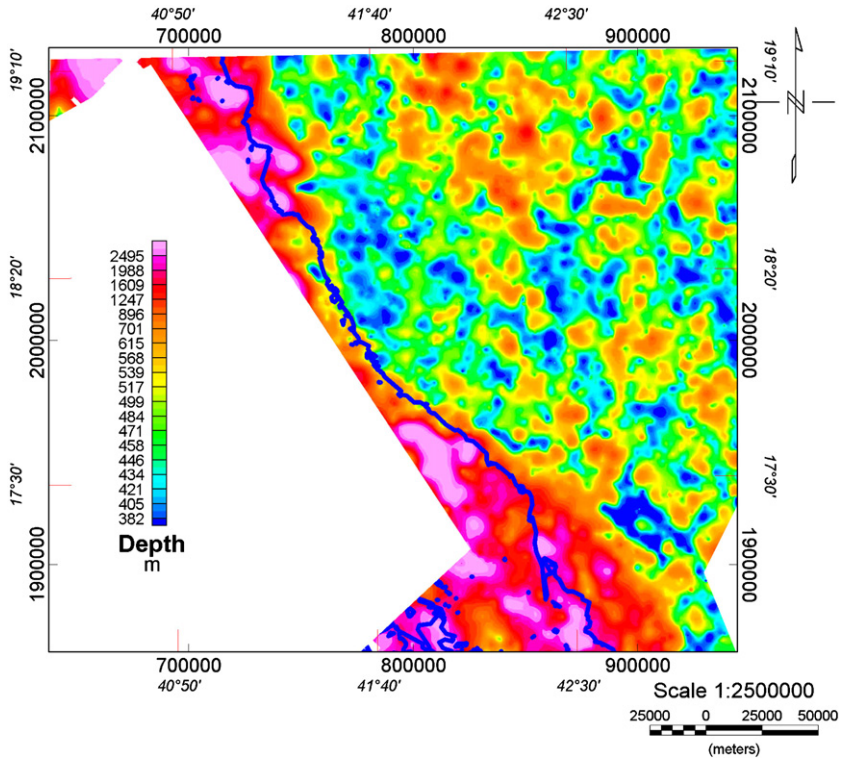

Figure 10. Local wavenumber (SPI) map based on the extension of complex analytical signal to estimate magnetic depths to the basement in the study area.

volcanic flows are present at the surface and subsurface and they represent a common obstacle facing groundwater drilling in some localities, where in other localities they cover the groundwater bearing formation.

The RTP and regional magnetic maps (figures 3 and 4) show a large and broad low magnetic anomaly that dominates the southeastern side of the study area, which is interpreted as a large structural basin filled mainly with the Sabya Formation, which consists of quartzite, quartz pebbles, conglomerate, limestone and greywakes (Blank *et al* 1985). This broad, low magnetic anomaly is superimposed by small circular and linear high magnetic anomalies which correlated to granite, syenite, monzogranite and gabbro and granodiorite intrusions (Fairer 1985). This basin and the Sabya Formation extend to the Yemen in the south (Blank *et al* 1985) where the NW trending faults and in-between fault-bounded grabens act as subsurface conduits for groundwater that receives feeding/recharging from the annual rainfall and/or the deep fossil aquifers from the south. Therefore, this basin is expected to be a good host for groundwater aquifers and hence a promising site for hydrogeological investigation. The Bouguer gravity shows that this basin is superimposed by a NW high trending anomaly which is faint on the regional magnetic map, which indicates that a high density of low magnetic intrusions dissects this basin.

A mosaic of narrow, elongated high magnetic anomalies extends in the NW direction and dominates the western side of the RTP and regional magnetic anomaly maps (figures 3 and 4). These anomalies indicate NW trending fault-bounded blocks that are intruded by Tertiary gabbro and diabase sheeted dyke swarms. These dykes have been intruded along the fault planes and extend parallel to the common fault trends in the area. Most of these are mafic dykes of a Tihamat Asir complexity which extend along the eastern margin of the coastal plain. These sheeted dyke swarms could play a role in preventing the sea-water intrusion from affecting the expected groundwater aquifer of the Sabya Formation, which filled the above mentioned interpreted basin. On the other side, these dykes delimit the faulted bounded troughs which are filled with a thick sequence of clastic sedimentary rocks, which, more probably, host a shallow groundwater aquifer.

The depths and locations of the magnetic sources are estimated using different analysis techniques (Euler, SED, HG and SPI). The results are compared and correlated and the consistent solutions are considered in the joint interpretation. The results (locations and depths) obtained from the analysis methods are presented in the figures 5 and 10, which show that the depth to the basement in the study area ranges from nearly 300–2500 m. The depth to the basement increases towards the Red Sea where the depth to the basement reaches 2500 m. Locally, towards the north and south, there are two basins where the depth to the basement reaches 900 m.

It is important to note that the main challenge when interpretating the magnetic data is the presence of the different basaltic intrusions at different depths in the study area. The form of these basaltic intrusions varies from intrabasement, as indicated in the southeastern side of the study area, to surface basaltic flow at the northwestern side of the study area. Therefore, great care was taken when interpretating the magnetic data to avoid any ambiguity. In addition, in order to avoid any masking effect from the surface basaltic flow, the structural interpretation of the magnetic data was done using

the regional magnetic anomaly data, i.e. after the removal of the surface basaltic effect.

6. Conclusions

It can be concluded that the groundwater aquifers in this coastal area are mainly affected and controlled by the Red Sea rift and the related faulting and volcanicity. The subsurface structures trend mainly in the NW with cross-cut NE trending faults, as inferred from the potential data used. The NW trending faults resulted in a mosaic of fault-bounded grabens on the eastern margin of the coastal plain. These faults and the resulting grabens could play a role as underground conduits for groundwater that receive feeding/recharging from the annual rainfall and/or the deep fossil aquifers in the south. On the other side, the NW faults are intruded by dykes of the Tihamat Asir complex, striking parallel to the fault trends in the region. These dykes could act as a sealing wall, which could prevent the sea water from intruding on the groundwater aquifer to the east. The present results indicate the possible existence of a large structural basin which extends to the southern border of the study area. This basin is bounded with NW and NE trending faults and is expected to be a good host for groundwater aquifers and hence a promising site for hydrogeological investigation.

Acknowledgment

This work was supported financially by the National Plan for Science, Technology and Innovation (NPST) program, King Saud University, Saudi Arabia (project no 09-WAT922-02).

References

Basahel A, Bahafzalla A, Mansour H and Omara S 1983 Primary structures and depositional environ of the haddat ash sham sedimentary sequence, northwest of Jeddah, Saudi Arabia *Arab Gulf J. Sci. Res.* **1** 143–55

Bird D 1997 Interpreting magnetic data: geophysical corner AAPG Explorer (May 1997)

Blakely R J and Simpson R W 1986 Approximating edges of source bodies from magnetic or gravity anomalies *Geophysics* **51** 1494–8

Blank R, Johnson P, Gettings M and Simmons G 1985 *Explanatory Notes to the Geologic Map of the Jizan Quadrangle* (Jiddah, Saudi Arabia: Deputy Minister for Mineral Resources) p 24

Cordell L 1979 Gravimetric expression of graben faulting *New Mexico. Geol. Sot. Guidebook: Santa Fe Country and the Espanola Basin, 30th Field Conf. (New Mexico)* pp 59–64

Fairer G M 1985 *Geologic Map of Wadi Baysh Quadrangle* (Jiddah, Saudi Arabia: Deputy Minister for Mineral Resources) sheet 17F, scale 1 250,000

Greenwood W 1985 *Geologic Map of the Abha Quadrangle* (Jiddah, Saudi Arabia: Deputy Minister for Mineral Resources) sheet 18F, scale 1 250,000

Hussain M and Ibrahim K 1997 Electric resistivity, geochemical and hydrogeological of Wadi deposits, Western Saudi Arabia *J. King AbdelAziz Univ. Earth Sci.* **9** 55–72

Mogren S, Batayneh A, Elawadi E, Al-Bassam A, Ibrahim E and Qaisy S 2011 Aquifer boundaries explored by geoelectrical measurements in the Red Sea coastal plain of Jazan area, Southwest Saudi Arabia *Int. J. Phys. Sci.* **6** 3768–76

Phillips J D 1998 Processing and interpretation of aeromagnetic data for the Santa Cruz basin—Patahonia mountains area *US Geological Survey Open-File Report* 02-98 (South-Central Arizona)

Prinz W 1984 *Geologic Map of the Jibal Hai'l Quadrangle* (Jiddah, Saudi Arabia: Deputy Minister for Mineral Resources) sheet 17E, scale 1 250,000

Reid A B, Allsop J M, Granser H, Millett A J and Somerton I W 1990 Magnetic interpretation in three dimensions using Euler deconvolution *Geophysics* **55** 80–90

Smith R S, Thurston J B, Ting-Fan D and MacLeod I N 1998 ISPI - the improved source parameter imaging method *Geophys. Prospect.* **46** 141–51

Thompson D T 1982 'EULDPH' a new technique for making computer-assisted depth estimates from magnetic data *Geophysics* **47** 31–7